where a is the lattice parameter. The sum over i was carried out on an IBM-7094 digital computer and included 35 000 atoms.

If we are considering a powder, we must average over all directions. We find that the average value of A_{qr} is independent of q and is given by

$$A_{qr}^2=\frac{\gamma^4\hbar^4}{4}\frac{4}{5}\frac{1}{(3a^2/4)^3}=\frac{\gamma^4\hbar^4}{4}\frac{1.8963}{a^6}. \quad \text{(A7)}$$

Now

$$\sum_i A_{ir}A_{iq}=\frac{\gamma^4\hbar^4}{4}\sum_i\frac{(1-3\cos^2\theta_{ir})(1-3\cos^2\theta_{iq})}{R_{ir}^3R_{iq}^3}, \quad \text{(A8)}$$

where $\cos\theta_{iq}$ is given by an expression analogous to Eq. (A3). Since we are considering only nearest-neighbor jumps, we have for one jump that

$$X_{iq}=X_{ir}+\tfrac{1}{2}a,$$
$$Y_{iq}=Y_{ir}+\tfrac{1}{2}a,$$
$$Z_{iq}=Z_{ir}+\tfrac{1}{2}a,$$

and

$$R_{iq}=[(X_{ir}+\tfrac{1}{2}a)^2+(Y_{ir}+\tfrac{1}{2}a)^2+(Z_{ir}+\tfrac{1}{2}a)^2]^{1/2}. \quad \text{(A9)}$$

Note that since we are averaging over a powder, all jumps are the same. When we average over a powder, we get

$$\sum_i A_{ir}A_{iq}=\frac{\gamma^4\hbar^4}{4}\sum_i\frac{1}{R_{ir}^3R_{iq}^3}\times\left\{-\frac{2}{5}+\frac{6}{5}\frac{(X_{ir}X_{iq}+Y_{ir}Y_{iq}+Z_{ir}Z_{iq})^2}{R_{ir}^2R_{iq}^2}\right\}. \quad \text{(A10)}$$

Evaluating this sum on the IBM computer, we obtain

$$\sum_i A_{ir}A_{iq}=(\tfrac{1}{4}\gamma^4\hbar^4)(4.2895/a^6). \quad \text{(A11)}$$

Therefore, we get for p

$$p=\frac{\left\{\frac{1}{8}\times 8\frac{\gamma^4\hbar^4}{4}\frac{1.8963}{a^6}+\frac{\gamma^4\hbar^4}{4}\frac{4.2895}{a^6}\right\}}{\frac{\gamma^4\hbar^4}{4}\frac{23.2336}{a^6}}=0.2663. \quad \text{(A12)}$$

PHYSICAL REVIEW VOLUME 137, NUMBER 1A 4 JANUARY 1965

Photoelectric Properties of Cleaved GaAs, GaSb, InAs, and InSb Surfaces; Comparison with Si and Ge

G. W. GOBELI AND F. G. ALLEN
Bell Telephone Laboratories, Murry Hill, New Jersey
(Received 14 August 1964)

Work function and photoelectric threshold, yield, and energy distributions are given for nearly perfect atomically clean (110) surfaces of GaAs, GaSb, InAs, and InSb of known doping cleaved in a vacuum of 10^{-10} Torr, and are compared with results on cleaved (111) Si and Ge. The spectral-yield curves are made up of one or more distinct linear portions. Each of these is interpreted as a direct optical excitation in the bulk for which **k** is conserved during emission, and the transitions are tentatively identified. GaAs and InAs, like Si, exhibit appreciable gaps (0.76 eV for GaAs) between the Fermi level and the top of the valence band at the surfaces and show only one linear rise in yield up to 6.3 eV. GaSb and InSb, like Ge, have the Fermi level coincident with the top of the valence band at the surface, and exhibit two different linear rises in yield. Surface states, while present in sufficient density to cause band bending, do not yield appreciable emission compared to valence-band states.

I. INTRODUCTION

THERE is relatively little literature concerning the photoelectric emission and work functions of the III-V compound semiconductors. This is partly due to the fact that these materials have become available in well defined single crystals only recently. The work reported by Haneman[1] and Haneman and Mitchell[2] on broken GaAs and InSb surfaces represents the total presently available. In view of the great interest in the III-V compounds the measurements of photoelectric emission spectra, emitted electron kinetic energy distributions and work functions which have been reported for atomically clean cleaved (111) Si[3] and Ge[4] have been extended in this work to the cleaved (110) surfaces of GaAs, GaSb, InAs, and InSb. The results are analyzed to give work functions, position of the Fermi level at the surface and some details concerning the band structure of the compounds.

[1] D. Haneman, Phys. Chem. Solids **11**, 205 (1959).
[2] D. Haneman and E. W. J. Mitchell, Phys. Chem. Solids **15**, 82 (1960).
[3] F. G. Allen and G. W. Gobeli, J. Appl. Phys. **35**, 597 (1964).
[4] G. W. Gobeli and F. G. Allen, in *Proceedings of the International Conference on the Physics and Chemistry of Surfaces* (North-Holland Publishing Company, Amsterdam, 1964).

II. APPARATUS AND EXPERIMENTAL PROCEDURE

The apparatus and cleaving technique are the same as those described earlier in detail for cleavage of silicon[5–7] in which long bar samples could be repeatedly cleaved in a vacuum of 2×10^{-10} mm Hg. An auxiliary storage tray was incorporated into the experimental tube which allowed all four of the compound crystals to be transferred in turn to the cleavage stem without opening the apparatus to air.

Whereas Si and Ge cleave along the (111) plane, the III-V compounds cleave along (110) planes. Several attempts were made to produce (111) and $(\overline{1}\overline{1}\overline{1})$ cleavages in room air but no usable (or detectable) cleavages in these planes could be obtained. All samples were cut with their length along the (110) direction within 2°, lapped and then etched with a solution of 10% Br_2 in methanol. The L-shaped cross section, which has promoted excellent cleavages in Si [5] and Ge,[4] was employed. Cleavages of excellent quality, often extending over the entire cross section were produced more readily than with Si and Ge, and in fact the L-shaped cross section may not be needed for the III-V's. Electron microscopic examinations with a resolution of 30-50 Å were made on direct cast replicas and showed the same type of terraced structure observed for Si. However, the present III-V surfaces were about one order of magnitude more perfect than for Si, i.e., plateaus 10 000 to 30 000 Å separated by steps some 40–100 Å high.

Low-energy electron diffraction studies of cleaved (110) faces of GaAs, GaSb, InAs, and InSb indicate very minor reconstruction of the surface compared to the bulk structure and show *no* evidence of a phase change upon heating to within ~50°C of the melting temperatures.[8] The quality of the diffraction pattern also indicated that the surfaces produced by cleavage in these materials is of unusually high quality on an atomic scale.

Work function was measured by the Kelvin contact potential difference method referred to a clean single-crystal tungsten reference, whose true work function was determined from photoelectric emission measurements. The accuracy of the work function value on an absolute basis is estimated as ±0.05 eV. For the freshly cleaved (110) surfaces of good quality the work function varied by no more than ±0.01 eV over the entire usable surface area (2×8 mm).

Photoelectric-emission current was measured as current emitted from the sample face with all other conductive tube elements including the cleavage clamps and support mechanism serving as collectors. For the retarding potential experiments to measure total energy distributions, samples were inserted into a mesh enclosure through an aperture that gave 0.005-in. clearance around the sample cross section. Fringe fields between the cleaved and dirty surfaces of the sample were minimized by placing the front face of the sample coplanar with the inside face of the aperture. Empirically it was found that this positioning minimized the total spread of the electron distribution; and for crystals in which photoemission was observed for photon energies equal to the work function φ, the total spread was equal to $h\nu-\varphi$ within 0.10 eV. The enclosure was covered with an evaporated layer of gold to minimize work function variation over its surface.

A linear voltage ramp for the collector was produced by integrating a constant (battery) voltage with an electronic operational amplifier. The photoemission current was measured by a vibrating-reed electrometer and the $I-V$ characteristic could be displayed directly on an $X-Y$ recorder. Alternatively the electrometer output served as input to an operational amplifier differentiator in which case dI/dV versus V was displayed on the $X-Y$ recorder. (Actually, dI/dt was measured, but since $V=Kt$, $K(dI/dV)$ resulted.) With suitable filtering, structure with half-width of ~0.2 eV in the kinetic-energy distributions could be reliably resolved when the saturation current was as little as 3×10^{-13} A.

As before, the light intensity incident on the samples was measured by comparison with a CsSb phototube calibrated by Apker and Taft. Corrections for reflectivity losses as a function of photon energy have been made from the data of Phillip and Ehrenreich,[9] where available. For GaSb a constant reflectivity of 0.5 was assumed. It should be noted that these experiments were carried out with a Bausch and Lomb 500-mm grating monochromator. This is an unevacuated instrument and therefore the present measurements were limited in photon energy to the air cutoff limit, i.e., photon energies less than $\sim h\nu=6.4$ eV, or $\lambda>1950$ Å.

III. RESULTS AND DISCUSSION

Figure 1 shows the measured photoelectric-yield spectra in electrons per absorbed photon for cleaved GaAs, GaSb, InAs, InSb, Si, and Ge. The latter two are included for purposes of comparison. The spectra are for the (110) faces of the III-V compounds and for the (111) faces of Ge and Si. Empirically it has been found that the low-energy points obey an approximate cube law (see below) and the inset shows such a cube root plot for each material. The heavy arrow indicates the work function for each sample as measured by the Kelvin method. The most striking general features of these data are that the materials investigated fall into two distinct groups. One group (GaAs, InAs, Si) in the upper half of Fig. 1 show photoemission only for

[5] G. W. Gobeli and F. G. Allen, Phys. Chem. Solids **14**, 23 (1960).
[6] F. G. Allen and G. W. Gobeli, Phys. Rev. **127**, 150 (1962).
[7] G. W. Gobeli and F. G. Allen, Phys. Rev. **127**, 141 (1962).
[8] A. U. Mac Rae and G. W. Gobeli, J. Appl. Phys. **35**, 1629 (1964).
[9] H. R. Phillip and H. Ehrenreich, Phys. Rev. **129**, 1550 (1963).

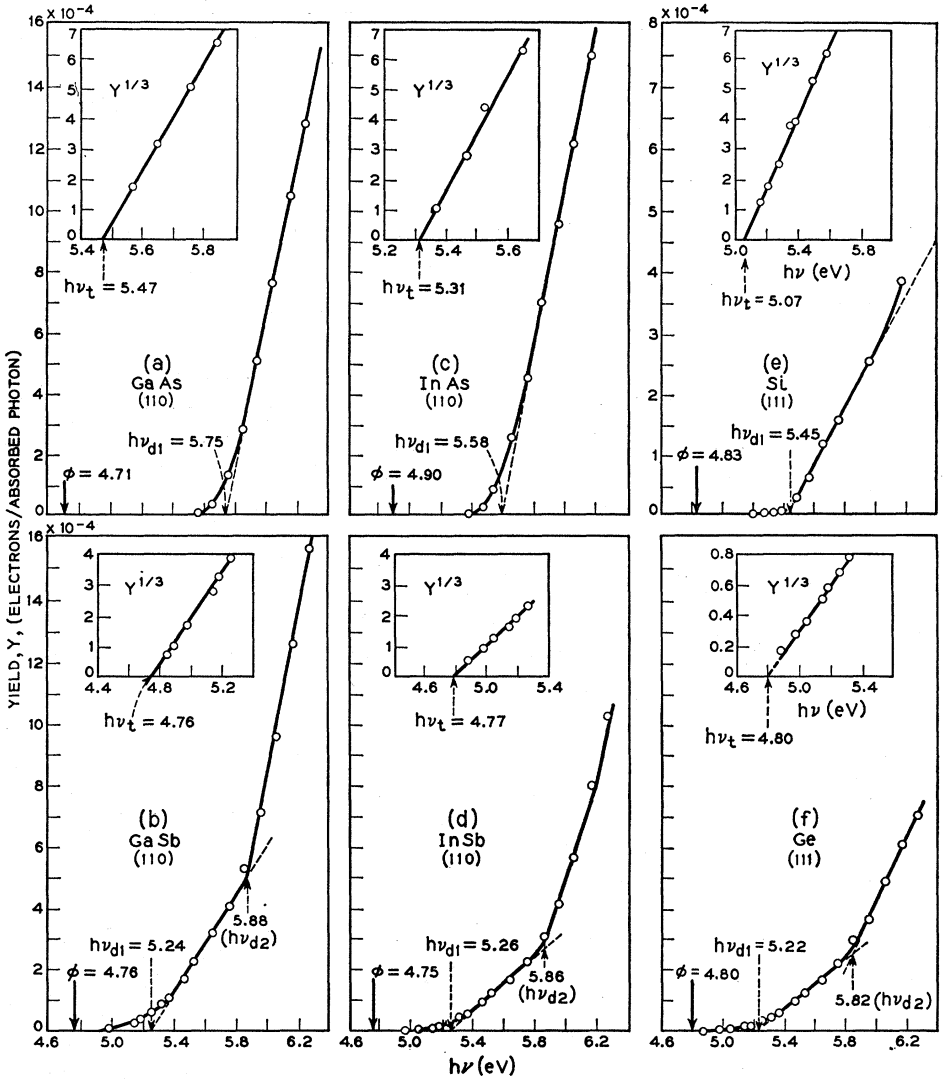

FIG. 1. Photoelectric yield versus photon energy for cleaved (a) GaAs, (b) GaSb, (c) InAs, (d) InSb, (e) Si and (f) Ge. Insets show (yield)$^{1/3}$ versus $h\nu$.

photon energies appreciably higher than the work function and have a single characteristic for photon energies up to $h\nu = 6.4$ eV. The second group (GaSb, InSb, Ge) in the lower half of Fig. 1 show photoemission for photon energies very close to the work function and exhibit a "break" in the yield characteristic at $h\nu \approx 5.8$ eV.

First, the establishment of Fermi level position at the surface of all the samples is necessary in order to determine what effects, if any, exist in the yield spectra due to band bending and bulk doping.[6,7] Therefore attention must be focused on the low-photon-energy region of each curve and on the measured work functions.

The location of the Fermi level in the bulk is established by measurement of the bulk electrical properties of the particular crystals used in the photoelectric and work function measurements. After cleavage and measurements were completed, the crystals were removed, and the conductivity at each cleavage surface was measured with a four-point probe apparatus. These measurements were compared with the conductivity values of the crystal prior to the experiment. In all cases the electrical properties were essentially unchanged and thus the original carrier concentrations determined from Hall effect measurements were used to calculate the bulk Fermi levels. The results of these measurements are listed in columns 2, 3, 4 of Table I as well as being illustrated by the band diagrams of Fig. 3. The Fermi level position at the surface is established by determining the energy difference, first: from the vacuum level to the Fermi level, i.e., the work function ($E_{\text{vac}} - E_F = \varphi$); and second: from the vacuum level to the valence-band edge at the surface, i.e., the photoelectric threshold ($E_{\text{vac}} - E_V = \Phi$). The Fermi level position relative to the valence band edge at the

TABLE I. Summary of data and results on the samples used.

(1) Sample	(2) ρ Ω-cm	(3) N_D, N_A cm^{-3}	(4) (E_F-E_V) bulk	(5) $E_G=(E_C-E_V)$	(6) φ (eV)	(7) $\Phi=h\nu_t$	(8) $h\nu_{d1}$	(9) $h\nu_{d2}$	(10) $\delta=\Phi-\varphi$	(11) $\chi=\Phi-E_g$	(13) Ionicity
GaAs(110)	0.08(*n*)	2×10^{16}	1.35	1.40	4.71	5.47	5.75		0.76	4.07	0.51
GaSb(110)	0.07(*p*)	1.2×10^{17}	0.08	0.70	4.76	4.76	5.24	5.88	0	4.06	0.33
InAs(110)	0.01(*n*)	2.4×10^{16}	0.31	0.36	4.90	5.31	5.58		0.41	4.90	0.56
InSb(110)	0.02(*n*)	5.5×10^{14}	0.12	0.18	4.77	4.77	5.26	5.86	0	4.59	0.42
Si(111)	250 (*p*)	2×10^{16}	0.25	1.09	4.83	5.10	5.45		0.27	4.01	...
Ge(111)	0.02(*p*)	4.0×10^{17}	0.05	0.67	4.80	4.80	5.22	5.82	0	4.13	...

surface is defined as

$$\delta=\Phi-\varphi.$$

The work function φ is obtained directly from the Kelvin contact potential difference experiment and unambiguously give the values listed in column 6, Table I within the absolute error of ±0.05 eV.

The identification of Φ must be made from the photoelectric emission data near threshold since the valence-band edge should manifest itself as the uppermost filled electronic states of very high density. Although the density starts from zero at the band edge, it increases rapidly upon moving deeper into the valence band, and an appropriate extrapolation should reveal its location.

The yield near threshold for all materials was plotted with various power-law assumptions in order to establish the spectral characteristic. A typical example of such data is shown in Fig. 2 where the yield for a GaAs sample is plotted to the $\frac{1}{2}$, $\frac{1}{3}$, and $\frac{1}{4}$ power versus $h\nu$. These results, and those for other samples, indicate that the cubic power most closely represents the data and that the yield in this region obeys the relation

$$Y\propto(h\nu-h\nu_t)^{3\pm\frac{1}{2}}, \qquad (1)$$

where $h\nu_t$ is defined as the extrapolated threshold value of the cube root plots such as shown in the insets of Fig. 1. The cube law appears to be reliable to $\pm\frac{1}{2}$ in the exponent. It should be noted that the threshold $h\nu_t$ obtained by extrapolation depends slightly on the power law assumed. For example in Fig. 2 the threshold varies from 5.56 eV for the $Y^{1/2}$ extrapolation to 5.45 eV for the $Y^{1/4}$ extrapolation. This however represents an error of only ±0.05 eV from the cubic-law extrapolation and is thus within the experimental error of the experiment.

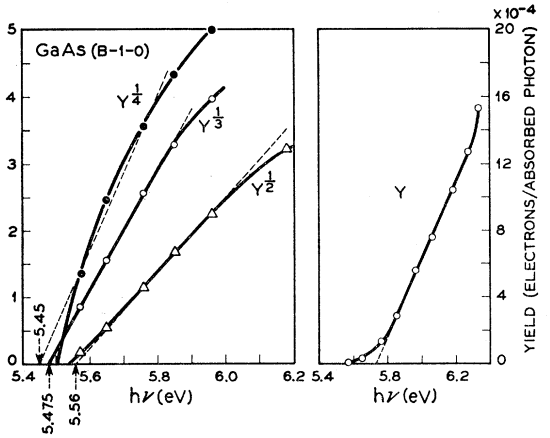

FIG. 2. Power-law fit for photoelectric yield near threshold for GaAs.

The theory of photoelectric emission[10] predicts various power laws for the yield spectrum depending upon the mechanism responsible for such emission. For the yield near threshold the following processes and resultant power laws could account for the emission. For a discussion of these processes and derivation of the power laws, the reader is referred to Ref. 10.

(1) Volume indirect optical excitation:

$$Y\propto(h\nu-h\nu_t)^{5/2}.$$

(2) Volume state—surface as momentum absorber: $Y\propto(h\nu-h\nu_t)^{3/2}$ for perfect surface; $Y\propto(h\nu-h\nu_t)^{5/2}$ for scattering surface.

(3) Surface band states—direct optical excitation: $Y\propto(h\nu-h\nu_t)^{3/2}$, indirect excitation: $Y\propto(h\nu-h\nu_t)^{5/2}$.

(4) Surface imperfection states—distributed in energy: $Y\propto(h\nu-h\nu_t)^2$.

It is certainly possible that more than one of these processes could contribute to the yield near threshold and if such is the case, the mixing of the processes in varying ratios with different power laws would yield an effective power law that is some average of the individual processes. Furthermore, while the cleaved surfaces are of high quality they are not perfect. There is thus a contribution to the yield from very small areas of slightly lower and higher than average threshold. The addition of these in the total yield always *increases* the curvature of the experimental plot near threshold, giving too large an exponent of $(h\nu-h\nu_t)$. It is thus difficult to establish the physical mechanism which is responsible for the yield near threshold from its power-law dependence, and attempts to do so, especially on less than ideal surfaces, are open to

[10] E. O. Kane, Phys. Rev. **127**, 132 (1962).

question.[11] However, because the threshold is determined from an extrapolation of the cube law fit to the lowest measurable yield points, it is felt that it should give the energy difference between E_{vac} and the uppermost filled electronic states of appreciable density within the above described accuracy of ± 0.05 eV.

In a previous paper[7] the authors identified the cube-law region of the yield curve for silicon as being due to phonon-assisted volume indirect optical transitions. Polarization experiments[12,13] on germanium have since shown that the directional yield is strongly sensitive to photon-polarization angles at normal incidence for photon energies just above $h\nu_t$ and in the cube-law region. This result is incompatible with the indirect transition hypothesis. Such transitions would randomize the tangential $\mathbf{k}$ vector for emitted electrons and thus destroy their "memory" of their point of origin in $\mathbf{k}$ space and hence of the photon-polarization angle used.

The polarization sensitivity in this photon energy range can be explained if the excitation occurs sufficiently close to the surface that appreciable normal momentum transfer to the surface occurs during the act of absorption, i.e., the analogue of classical "surface" photoelectric emission. In this case tangential momentum $\mathbf{k}_t$ would be conserved, but normal momentum $\mathbf{k}_n$ could be arbitrary and thus allow transitions from states up to the top of the valence band. In this case the identification of $h\nu_t=\Phi$ can be justified.

The polarization sensitivity could also be preserved in case of excitation from surface states due to the high symmetry of a (111) surface.[13] Since the polarization sensitivity varied smoothly (and did not change sign) from just above $h\nu_t$ up to above the direct threshold where volume processes surely dominate,[12] the surface-state explanation seems unlikely. Further arguments follow that suggest surface-state emission is not important, so that the most likely explanation of the yield mechanism just above threshold is presently thought to be normal momentum takeup by the surface. The discrepancy between Kane's predicted $\frac{3}{2}$ power for this process for a perfect surface and the experimental value of $3\pm\frac{1}{2}$ may be due to the admixture of some scattered electrons (a $\frac{5}{2}$ power), plus the tendency of the experiment to yield too high an exponent.

The identification of $\Phi=(E_{vac}-E_v)_s$ as being equal to $h\nu$ is difficult to prove since it is possible that appreciable photoelectric emission could originate from electrons in filled surface states which are located in high densities in the forbidden energy gap. This point clearly requires considerable discussion: First there is strong evidence from surface Fermi-level clamping versus bulk doping for Si,[6] Ge,[4] and GaAs (below) that surface state densities of *at least* 10^{14}, 10^{13} and 10^{12} per cm, respectively, exist in the forbidden band for these cleaved surfaces. Now emission from valence band states in the volume proceeds from a depth of about 25 Å for Si,[7] or about 10 atomic layers. Since the valence band is of the order of a few volts in width with $\sim$ one state per atom, the number of available valence band states for emission within a few tenths of an eV of threshold is roughly one monolayer, or $\sim 10^{15}$ per cm^2. Hence if photoemission were equally efficient from surface states and valence-band states, one would expect to see at least $\frac{1}{10}$ as much emission from surface states as from volume states in silicon. This crude approach has of course neglected the specification of upper energy states into which transitions can occur.

If present, surface state emission could give a measured value of the photothreshold Φ smaller than its true value by at most several tenths of an eV. The following experimental results indicate, however, that such emission is usually negligible compared to volume emission for the present samples.

(1) For Si, independent measurements of surface conductivity of the freshly cleaved surface confirm the flatband[14] location of the Fermi level as being ~ 0.30 eV above E_v.[15] This value added to the measured work function of such a sample of 4.83 eV gives the value of $\Phi=5.13$ eV which is equal within experimental accuracy to the value of $h\nu_t=5.07$ eV obtained in Fig. 1(e) above. This suggests the identity $h\nu_t=\Phi$.

(2) For InAs [Fig. 1(c), 3(c)] the extrapolated value $h\nu_t=5.31$ eV and the work function $\varphi=4.90$ eV gives $\delta=0.41$ eV which is equal within the experimental error tc the forbidden energy gap of 0.36 eV. The surface could not have been more than a few kT degenerate n type, or appreciable emission would have arisen from filled conduction band states just beneath the Fermi level. Hence we have an energy range of $\sim$ one energy gap extending downward from some level at or below the bottom of the conduction band over which no appreciable emission occurs. Since emission can be expected to set in strongly as soon as the top of the valence band is reached, the conclusion must be that for InAs, at least, no appreciable surface state emission occurs. The threshold seen is thus indeed the valence band maximum, i.e., $h\nu_t=\Phi$.

(3) The cube-root law extrapolates to a value $h\nu_t=\varphi$ for InSb, GaSb, and Ge. For Ge this equality holds true for a bulk doping range from 2×10^{19} holes/cm^3 to 1×10^{18} electrons/cm^3. The clear implication is that the Fermi level at the surface of these materials always lies at the valence-band edge. The fact that GaAs, InAs, and Si all have $h\nu_t>\varphi$ by several tenths of a volt and yet also give a cubic power law near threshold

[11] J. J. Scheer and J. van Laar, Phys. Letters **3**, 246 (1963).
[12] G. W. Gobeli, F. G. Allen, and E. O. Kane, in Proceedings of International Conference of Semiconductor Physics, Paris, 1964 (to be published).
[13] G. W. Gobeli, F. G. Allen, and E. O. Kane, Phys. Rev. Letters **12**, 94 (1964).
[14] The "flat band" condition results when bulk doping is chosen so that the Fermi-level position relative to the bands in the bulk is just that required at the surface for zero surface-state charge.
[15] P. Handler, Appl. Phys. Letters **3**, 96 (1963).

implies that the threshold mechanisms are the same for all six materials. The identity of $h\nu_t=\Phi$ most easily accounts for these observations since the valence-band edge should be qualitatively similar for all six materials.

(4) For GaAs, InAs, and Si no emission was observed for a range of 0.76, 0.41, and 0.27 eV beneath the Fermi level. Since for both GaAs and Si there is evidence from band bending of high surface-state densities in the forbidden band beneath the Fermi level, one can conclude that the efficiency for emission from any surface states lying in the above ranges is very low compared to that for valence band states. (It is expected, however, that a search for such emission with a high sensitivity detector will reveal its presence.)

(5) Although the basic mechanism and origins of the cubic component may be in doubt, the identity of the linear component at somewhat higher photon energies is more firmly established. We will now show that this puts a further limit on the uncertainty in the value of Φ. From its dependence upon band bending beneath the surface as bulk doping is changed, the linear component is clearly due to a volume process.[7] From its spectral dependence (linear), high efficiency, and from polarization experiments it can further be identified as being due to a direct-optical excitation in the volume. Except in very special circumstances, that of excitation occurring in a very small volume centered in the Brillouin zone at $k=(000)$, the exciting photon will impart some kinetic energy to the hole which is created in the act of absorption. That is, the direct absorption process satisfies

$$E(\mathbf{k})_{\text{final}}-E(\mathbf{k})_{\text{initial}}=h\nu \tag{2}$$

and

$$\text{kinetic energy of hole}=E_V(000)-E(\mathbf{k})_{\text{initial}}. \tag{3}$$

Such a transition is shown in Fig. 4(a), as $h\nu_{d1}$. Therefore, clearly in any case the linear extrapolation[16] yields a threshold $h\nu_d$ which is an upper limit on the true value of Φ. Note that $h\nu_d$ would be just equal to Φ in the special case where the transition can take place at $\mathbf{k}=(000)$.

The above arguments permit clear absolute bounds to be set upon Φ, specificially,

$$h\nu_d\geq\Phi\geq h\nu_t. \tag{4}$$

Since the valence band for both Ge and Si (and presumably the III-V's considered here) varies by more than 1 eV as $\mathbf{k}$ moves from (000) to the zone boundary, it is expected that for likely $\mathbf{k}$ values at the direct transition threshold

$$h\nu_d-\Phi\sim\text{several tenths of an eV}.$$

From Table I, columns 7 and 8, we see that the whole uncertainty range in (4) for all six semiconductors lies in the range

$$h\nu_d-h\nu_t=0.28\text{ eV (GaAs) to }0.49\text{ eV (InSb)}.$$

The value of Φ is thus set definitely within quite narrow bounds. Furthermore, that the entire range is of the order of the expected separation of $h\nu_d$ and Φ suggests that Φ lies very close to its lower bound $h\nu_t$ and hence that surface states have not separated Φ and $h\nu_t$ by more than perhaps one or two tenths of an eV.

In light of the above listed arguments the identity will now be made in this paper that $\Phi=h\nu_t$. The extent of the uncertainty is clearly limited by Eq. (4). Hence Φ must lie between the value assigned to it in column 7, Table I (defined as $\Phi=h\nu_t$) and the value assigned to the direct transition threshold $h\nu_{d1}$ in column 8.

Using the data of Table I through column 7, the value of δ and χ given in columns 10 and 11 are obtained. χ, the electron affinity, is defined as $(E_{\text{vac}}-E_c)_s$. The band diagrams of Fig. 3 which show the band bending situations can now be drawn for each material. Note that band bending is negligible except for the GaAs samples. However, the doping level is sufficiently low in the GaAs that the bands bend by only $\sim$0.1 eV in the first 100 Å. The absorption depth for light of 5.5 eV in GaAs is $\sim$100 Å and would thus establish that any band-bending effects in the photoelectric yield spectra would be unobservable.

The charge Q_{ss} held in surface states on the GaAs surface can be computed from the known band bending. An approximate solution is given by the Schottky exhaustion formula

$$Q_{ss}^2=(Ke\Delta\psi_s(N_D-N_A))/2\pi,$$

where K is the static dielectric constant, $(e\Delta\psi_s)$ is the total bending $(E_v)_s-(E_v)_B\approx0.6$ eV from Fig. 3(a), and $(N_D-N_A)=2\times10^{16}$ cm^{-3}. The result gives

$$Q_{ss}\sim5\times10^{11}\ e\text{ units/cm}^2,$$

and since the surface states are not all filled we can safely say that the density of surface states must be

$$N_{ss}\geq10^{12}\text{ cm}^{-2}.$$

Now let us focus attention on the higher energy portions of the yield spectra. For photon energies appreciably greater than $h\nu_t$ a sharply rising linear component of emission is observed for all materials. For the second "family" of materials (GaSb, InSb, Ge) as noted above, a second linear component also enters near $h\nu=5.8$ eV. As has been discussed for Si[7,10] such linear yield spectra can be explained only by ascribing the yield to direct optical transitions in the volume followed by emission of the excited electron without subsequent scattering in the bulk or at the surface. This absence of scattering has been clearly confirmed for Si and Ge by polarization experiments.[13]

[16] Whether $h\nu_d$ should be taken at the linear extrapolation of yield to zero, at the merging point of the cubic and linear portions, or somewhere in between, will not be known until the cubic tail is understood. $h\nu_d$ and hence the uncertainty in (4) will be $\sim$0.15 eV larger than reported here if the second instead of the first alternative proves correct.

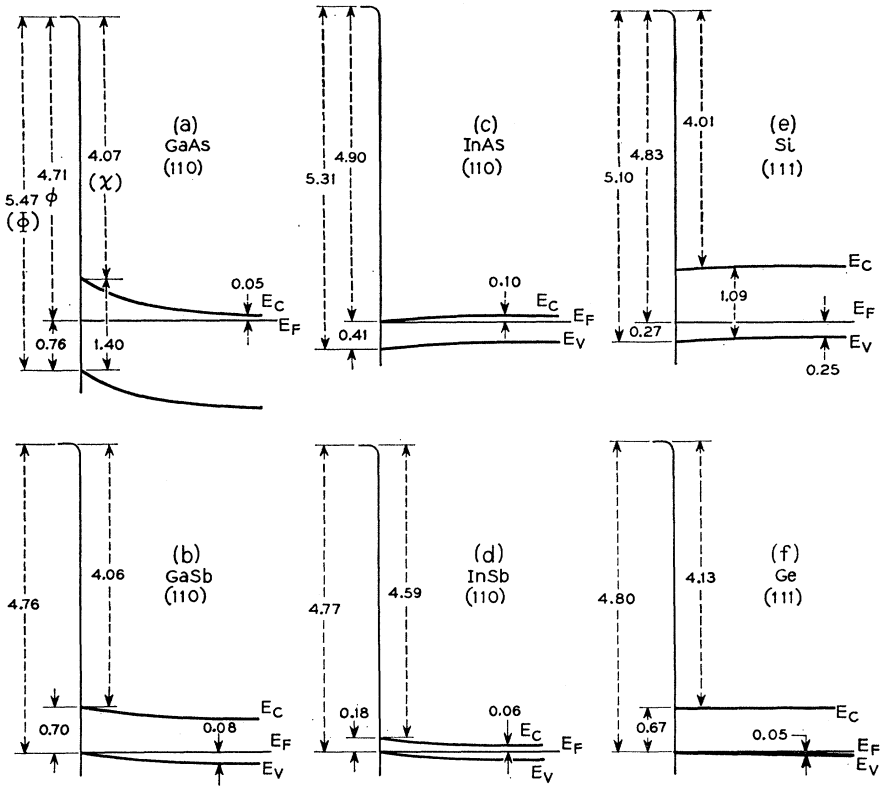

FIG. 3. Band diagrams for semiconductors having photoelectric spectra given in Fig. 1. (a) GaAs, (b) GaSb, (c) InAs, (d) InSb, (e) Si, (f) Ge.

The linear yield relations for the four III-V compounds shown in Fig. 1 indicates that they, like Si and Ge, exhibit direct optical excitation with **k** conservation followed by emission without scattering at least for the clean cleaved surface. This is in contrast to the non-direct transitions that Spicer has proposed[17] to explain the photoemission behavior of the IA-VB compounds, CdS and the alkali halides.

Near a photoelectric threshold the emitted electron must have small total kinetic energy upon emission into vacuum, and hence, small tangential kinetic energy $h^2k_t^2/2m_0$. But the above absence of scattering means that transverse momentum is conserved on passing through the surface, i.e., $(k_t)_{\text{outside}}=(k_t)_{\text{inside}}$. Hence, near threshold, $(k_t)_{\text{inside}}$ must be small. This means that the optical excitation which is effective in the emission process must occur for energy states having k vectors close to the (111) direction for Ge and Si or close to the (110) direction for the III-V's.[10] Since these directions in the crystals are high-symmetry directions, the E versus **k** diagrams have extrema along them. Hence a reasonable qualitative discussion of the effects on the yield spectra of the band structure properties can be carried out from an examination of the E versus **k** diagram from $k=0$ to the Brillouin zone boundary, moving along the (111) direction for Ge and Si and along the (110) direction for the III-V's.

Brust, Cohen, and Phillips, using the pseudopotential method, have calculated the energy band structure for Si shown in Fig. 4(a).[18,19] Figure 4(b) shows the energy versus x diagram of Fig. 3 on the same energy scale as for 4(a). The vacuum level is indicated on the E versus **k** diagram and the lowest energy states which can yield photoelectrons must lie at or above it. The lowest photon energy which can yield such emission via a direct transition for a (111) surface is indicated by the vertical arrow marked $h\nu_{d1}$. Theoretically this is the value obtained by the extrapolation of the linear yield component of Fig. 1(e) and has the value 5.45 eV. This requires that 0.35 eV of kinetic energy be given to the "hole" left behind in the valence band which is represented on the diagram as the energy difference between E_v at $k=0$ and the point of origin of the vertical arrow.

The E versus **k**[18,19] diagram for Ge, shown in Figs. 5(a) and (b), is qualitatively very similar to that for Si, the major difference being that the Γ_2' branch is considerably lower and the Γ_{15} branches are somewhat higher. Based on the interpretations of Sec. III, the vacuum level is placed 4.80 eV above E_v at $k=0$ and again the first direct transition threshold should lie along the (111) direction for a Ge(111) surface and is indicated as a vertical arrow $h\nu_{d1}$ with the value 5.22 eV. Note that the kinetic energy of the hole for this

[17] W. E. Spicer, Phys. Rev. Letters **11**, 243 (1963).

[18] D. Brust, M. L. Cohen, and J. C. Phillips, Phys. Rev. Letters **9**, 389 (1962).

[19] D. Brust, Phys. Rev. **134**, A1337 (1964).

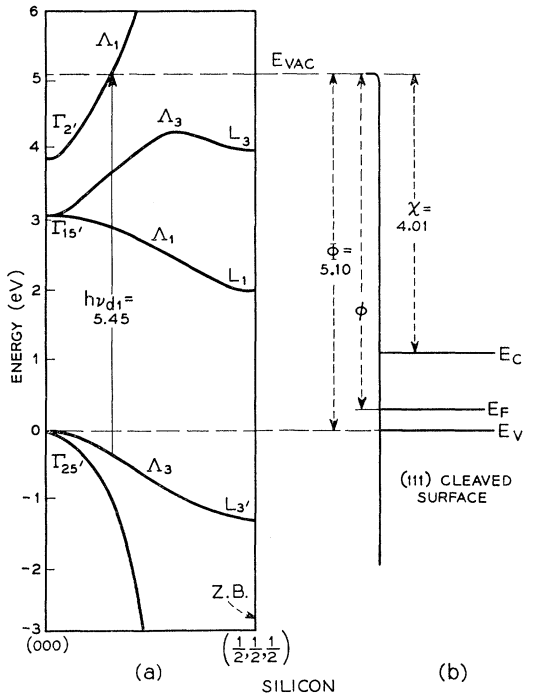

FIG. 4. (a) Energy versus $\mathbf{k}(111)$ for Si, (b) energy versus x for silicon at the cleaved (111) surface.

transition is ~0.4 eV. For Ge the L_3 branch extends to energies above E_{vac} and thus transitions into that branch from the valence band for larger $\mathbf{k}$ values (and high photon energies) should be possible. Such a transition is indicated by the vertical arrow $h\nu_{d2}$. Since it also is a direct-transition emission process its spectral characteristic will also be linear. The experimental data for Ge, Fig. 1(f), show a second linear characteristic with a threshold of 5.82 eV. It should be noted that the two linear components are additive for all energies and hence the threshold for the second process lies at the point of intersection of the two, as indicated. It must be stressed at this point that the exact shape of the bands in the $E-\mathbf{k}$ diagrams for both Si and Ge near these transitions are not yet known to better than several tenths of a volt. As far as they *are* known, however, they are consistent with the transitions indicated.

Further confirmation of the above interpretation can be found by examining the photoelectron kinetic energy distributions for Ge shown in Fig. 6(f). For photon energies $h\nu > h\nu_{d2}$, i.e., $h\nu > 5.82$, the curve $h\nu = 5.96$ shows a *low*-energy shoulder on the distribution. Electrons excited into the Λ_1 conduction band by photons of energy $h\nu > h\nu_{d2}$ will have a higher kinetic energy than those excited by the same energy photons into the Λ_3 conduction band at a larger $\mathbf{k}$ value. For $h\nu < h\nu_{d2}$ (but still greater than $h\nu_{d1}$), the curve for 5.76 shows that the low-energy group of electrons has disappeared leaving only the single asymmetrical peak. For $h\nu \cong h\nu_{d1}$, $h\nu = 5.37$, the distribution consists only of a single low-intensity symmetrical peak. These latter electrons which become the highest energy electrons for $h\nu = 5.76$ and 5.96 most probably are due to the cube-law tail emission process originating from initial states near the valence-band maximum.

This general explanation of a second direct transition threshold being responsible for the break observed in some spectra is also applicable to GaSb and InSb which show spectra very similar to that of Ge. (See yield spectra in Fig. 1 and distributions in Fig. 6.) Of course, in the case of the III-V's the band structure along the (110) $\mathbf{k}$ direction is of primary concern rather than along the (111) direction as in Ge or Si.

The band structure of these materials is far less well established, at present, than that for Ge and Si. It has been suggested[20] that the band structure of the III-V materials may be obtained by the pseudopotential method as a perturbation to the relatively well established group-IV semiconductor-pseudopotential parameters, particularly for GaAs, the atoms of which straddle Ge in atomic weights and numbers. This assumption implies therefore that the band structure in the (110) direction for the III-V compounds under investigation here [GaAs, GaSb, InAs, InSb], which all straddle or lie below Ge in the periodic table, should be somewhat similar to Ge along the (110) direction. Figure 5(a) shows the band structure of Ge along the (110) direction

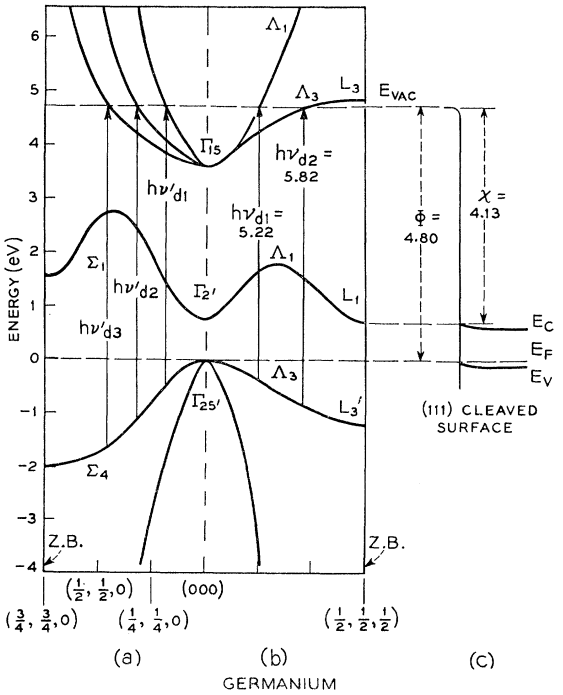

FIG. 5. (a) Energy versus $\mathbf{k}(110)$, (b) energy versus $\mathbf{k}(111)$, (c) energy levels near surface versus depth for cleaved (111) surface, all for Ge.

[20] M. L. Cohen (unpublished).

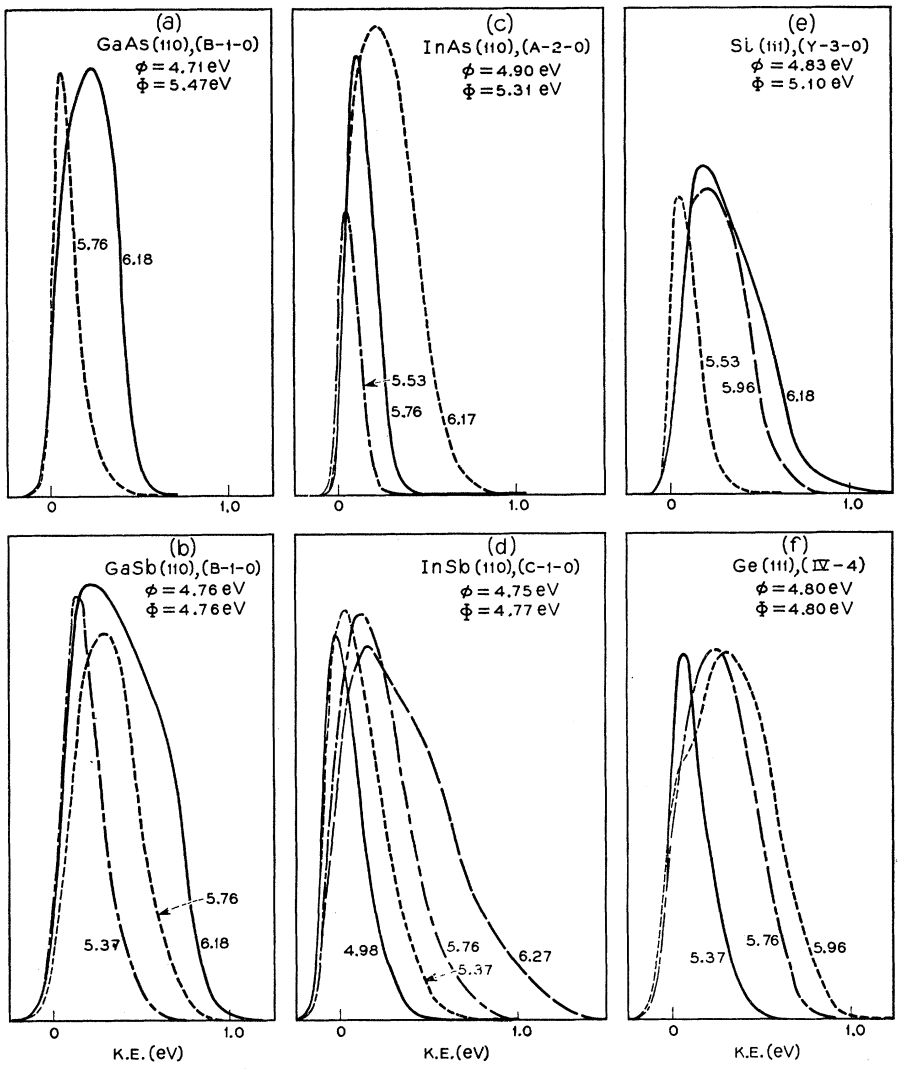

FIG. 6. Photoelectron kinetic energy distributions at various photon energies $h\nu$ from atomically clean cleaved surfaces of [a] GaAs (110), [b] GaSb ×(1$\bar{1}$0), [c] InAs(1$\bar{1}$0), [d] InSb(110), [e] Si(111), [f] Ge(111).

out to the zone boundary $(\frac{3}{4},\frac{3}{4},0)$, as well as the energy levels near the surface, 5(c). Note from Table I that E_{vac} for InSb and GaSb would lie only 0.03 and 0.04 eV, respectively, below that for Ge.

From consideration of this band structure alone one would expect to observe direct transitions [see Fig. 5(a)] at $h\nu_{d1}'\sim 5.3$ eV, $h\nu_{D2}'\sim 5.9$ eV, and $h\nu_{D3}'\sim 6.5$ eV, as the **k** vector moves out along the (110) direction and intercepts the three upper lying conduction bands in turn. Each transition will give rise to a new linear slope in the yield. It should be emphasized that the yield characteristic must be linear regardless of whether the transition is into a Γ type of upper conduction band as suggested here for the III-V compounds or into an L type band for the type-IV valence semiconductors.

These predicted transitions are remarkably close to the observed breaks in the experimental curves: namely, $h\nu_{d1}=5.24$ eV, $h\nu_{d2}=5.88$, $h\nu_{d3}=?$ (>6.3 eV, if existent) for GaSb (110); and $h\nu_{d1}=5.26$ eV, $h\nu_{d2}=5.86$ eV, $h\nu_{d3}=?$ (>6.3 eV if existent) for InSb (110). The highest energy threshold $h\nu_{d3}$ lies beyond the air cutoff limit of the experimental equipment at $h\nu\approx 6.3$ eV.

On the other hand, for GaAs and InAs, where $E_{\text{vac}}-E_v=5.47$ and 5.31, respectively, one would place the vacuum level about 0.5–0.7 eV higher in absolute energy on the same diagram. In that case we would predict that for these materials, $h\nu_{d1}'=5.9$ eV, $h\nu_{d2}'=6.8$ eV, $h\nu_{d3}'=7.2$ eV. In this case only the *lowest* of the thresholds is accessible to the present experiments ($h\nu<6.3$ eV). Thus on this tentative model one would expect that only a simple *single* linear yield characteristic would be observed, with a threshold photon energy of ~ 5.9 eV. The experimentally observed thresholds of 5.75 eV for GaAs and 5.58 eV for InAs are certainly reasonable considering the approximate nature of the estimates involved here. As in the case of Ge, the photoelectron-velocity distributions-yield confirmation of this multiple upper conduction-band characteristic in that

the distributions for GaSb and InSb show a double structure for $h\nu = 6.18$ eV ($h\nu > h\nu_{d2}$) and a single characteristic for $h\nu = 5.76$ eV ($h\nu < h\nu_{d2}$) as shown in Figs. 6(b) and (d), while those for GaAs and InAs shown in Figs. 6(a) and (c) show only a single characteristic at $h\nu = 6.18$ eV. Similar to the cases for Ge and Si, the asymmetry giving a high-energy "tail" in these cases also is ascribed to the photoelectrons produced in the cubic-law process.

It should be emphasized at this point that the experimental data demonstrate *only* the existence of two overlapping conduction bands at the vacuum level. The band structure diagrams of Figs. 4 and 5 are consistent with the data but this does not necessarily imply that the diagrams are correct as drawn. Also it is certainly true that a band structure similar to that of Fig. 5 should be calculated and plotted for each of the III-V's. Such work is in process[20] and preliminary results indicate that the general features of the band structure, at least near the vacuum level, are indeed similar to Fig. 5 although the separations $\Gamma_{25}' - \Gamma_{15}$ vary from 3.5 eV for InSb to 4.2 for GaAs.[21]

Further experimental evidence is at hand which adds credibility to the above explanation of the single and double linear yield curves. The above model predicts that for silicon, there *should* be a second break in the yield curve as soon as the energy barrier E_{vac}, is lowered beneath the top of the Λ_3 branch in the (111) direction [Fig. 4(a)]. When the energy barrier of a cleaved silicon surface is lowered by ~ 1.0 eV by adding ~ 0.1 monolayer of Cs, the single linear-yield law *does* change to a double linear characteristic with a break at $h\nu \approx 5.2$ eV, as predicted by the model. (This will be discussed more fully in a later publication.) Thus experimentally, there are now four examples available of double linear yield characteristics, all of which seem explainable by reasonable energy-band diagrams. It may be speculated that spectral yield curves from perfect crystal faces with no scattering may be found to consist quite generally of linear portions corresponding to various direct transitions.

A final comparison between the materials having type-I emission spectra (Si, GaAs, InAs) and those having type-II emission spectra (Ge, InSb, GaSb) can be made from Table I as follows: (a) the Fermi level at the surface is locked at the valence band edge for all type-II materials while a definite gap exists between E_F and E_V for type-I materials; (b) the values of the photothreshold Φ of type-II materials average 4.77 eV while those of type-I materials average 5.28 eV and this 0.5-eV difference is considerably larger than the spread in either group; (c) the ionicities of the two type-II compounds is 0.33 and 0.42 while those of the type-I compounds is 0.51 and 0.56[22]; (d) on the other hand the work functions of type-I and type-II materials show no significant correlations.

Further detailed information on the atomic and electronic configuration of the surface will be needed before explanations for differences in work functions and photothresholds can be given. Atomic structures of the cleaved surfaces have already been studied by low-energy electron diffraction for both the type-IV[23] and type-III-V[8] crystals. While the unit mesh of the surface structure of cleaved Ge and Si differs markedly from that of the bulk (111) planes and changes further upon annealing, the unit mesh of the cleaved III-V surfaces is identical to that of the bulk (110) planes and does not change upon annealing (*in vacuo*) up to the melting point.

Finally, it should be stressed that the present grouping into two "families" does not imply that any properties other than surface Fermi-level position, photoelectric threshold and certain features of the band structure near threshold for the clean surface are similar within families. Over-all similarity in band structure for two materials is much better indicated by the structure of the yield curves for the fully cesium-covered surfaces, where the E versus $\mathbf{k}$ diagrams can be sampled over a much larger energy range. This will be dealt with in later papers.

Note added in proof. The reflectivity values for GaSb should have been taken from M. Cardona,[24] in plotting the yield, Fig. 1(b), rather than assuming a constant value of 0.5. When this is done the curve is shifted downward by about 20%, but its shape and the threshold values are unchanged.

ACKNOWLEDGMENTS

The authors wish to thank E. O. Kane, J. C. Phillips, M. L. Cohen and D. Brust for helpful discussion, and A. A. Studna and F. R. Eyler for technical assistance.

[21] D. L. Greenaway, Phys. Rev. Letters **9**, 97 (1962).

[22] M. Haas and B. Henvis, Phys. Chem. Solids **23**, 1099 (1962).

[23] J. J. Lander, G. W. Gobeli, and J. R. Morrison, J. Appl. Phys. **34**, 2298 (1963).

[24] M. Cardona, J. Appl. Phys. **32S**, 2155 (1961).